Clim Dyn (2007) 28:517–531
DOI 10.1007/s00382-006-0195-8

Evaluating EOF modes against a stochastic null hypothesis

Dietmar Dommenget

Received: 19 April 2006 / Accepted: 15 September 2006 / Published online: 18 October 2006

Abstract In this paper it is suggested that a stochastic isotropic diffusive process, representing a spatial first order auto regressive process (AR(1)-process), can be used as a null hypothesis for the spatial structure of climate variability. By comparing the leading empirical orthogonal functions (EOFs) of a fitted null hypothesis with EOF modes of an observed data set, inferences about the nature of the observed modes can be made. The concept and procedure of fitting the null hypothesis to the observed EOFs is in analogy to time analysis, where an AR(1)-process is fitted to the statistics of the time series in order to evaluate the nature of the time scale behavior of the time series. The formulation of a stochastic null hypothesis allows one to define teleconnection patterns as those modes that are most distinguished from the stochastic null hypothesis. The method is applied to several artificial and real data sets including the sea surface temperature of the tropical Pacific and Indian Ocean and the Northern Hemisphere wintertime and tropical sea level pressure.

1 Introduction

One of the outstanding features of natural climate variability is that the variability is organized in specific spatial patterns. The El Niño Southern Oscillation (ENSO) mode is such an example. The accurate description of the spatial patterns associated to the modes is therefore an important issue in climate research.

Principal component analysis, also known as the empirical functions (EOFs) technique, is the most widely used method to identify these patterns. Often a single EOF mode is analyzed, assuming that this mode reflects a specific mode of climate variability with a well defined underlying physical mechanism.

The literature about EOF analysis, its statistical characteristics and alternative methods is vast and nearly intractable (an overview on EOF analysis is given in von Storch and Zwiers 1999; Jolliffe 2002 and references therein). Some important measures are given about the statistical uncertainties of EOF eigenvalues and patterns due to sampling limitations (North et al. 1982; Overland and Preisendorfer 1982). More important in the context of the interpretation of the statistical modes as reflections of underlying physical mechanism are studies focusing on the characteristics of EOF or other statistical modes of simple stochastic models, which may give some insight into the structures of the statistical modes as they may appear in observed physical systems (North 1984; Navarra 1993; Metz 1994; Gerber and Vallis 2005 and many others). North (1984) finds that the EOFs of some simple stochastic models driven by spatially white noise coincide with the eigen modes of the dynamic operator of the system. Navarra (1993), Metz (1994), Gerber and Vallis (2005) analyzed the atmospheric variability in simplified linearized models and found that the observed structures of meridional dipole variability can be explained by these simplified models.

Much of the discussion of the EOF-analysis is about its capability of presenting modes that reflect underlying physics. In general these discussions follow the

D. Dommenget (✉)
Leibniz-Institut für Meereswissenschaften,
Düsternbrooker Weg 20, 24105 Kiel, Germany
e-mail: ddommenget@ifm-geomar.de

concept of comparing the EOF-analysis with alternative definitions of statistical modes in order to point out which method works best (Richman 1986; Bretherton et al. 1992; van den Dool 2000; Aires 2002 and many others).

In Dommenget and Latif (2002a) three very simple modes of variability are used to construct a simple artificial example, in which the resulting EOF modes have very little in common with the three modes of variability used to create the multivariate problem, thus indicating that EOF modes do not necessarily reflect physical modes of a system. Although, this work only discusses the limitation of EOFs, the conclusions hold essentially for all statistical methods of defining modes of variability. The dilemma is that we like to use the concept of climate modes to understand climate variability, while the EOF-analysis or alternative statistical methods, which we use to define these, are pure mathematical concepts which will not necessarily detect the physical modes. The problem is to some degree due to the fact that the statistical modes are discussed without having a null hypothesis of how the statistical modes would look like if no outstanding climate modes exist. To evaluate the physical relevance of statistical modes it may therefore be helpful to formulate a null hypothesis for the statistical modes against which the observed modes can be compared.

Calahan et al. (1996) used a stochastic model with spatial correlation to compare the EOF-eigenvalues of rainfall variability over North America against, which essentially represents a spatial auto-regressive process of the first order. This approach is very similar to the null hypothesis used in analysis of time series. Here Hasselmann (1976) introduced the stochastic climate model as the null hypothesis for the time evolution of climate variables, which assumes, in its simplest form, an auto-regressive process of the first order.

In this paper it is illustrated how the formulation of a null hypothesis for the spatial structure of climate variability can help to evaluate the physical nature of EOF or other statistical modes and subsequently helps to identify outstanding patterns of climate variability.

The paper is organized as follows: In Sect. 2 a definition of climate modes and the concept of testing a stochastic null hypothesis are discussed. In Sect. 3 a null hypothesis for the spatial variability of climate variables is formulated. The procedure of how to evaluate EOFs against a stochastic null hypothesis is described in Sect. 4. The concept is applied to several artificial and real data sets in Sect. 5. The paper concludes with a discussion in Sect. 6.

2 Concepts

It is helpful to first discuss how climate modes could be defined and how limited such definitions may be. It is also instructive to illustrate how the concept of testing a stochastic null hypothesis is performed in time series analysis, which will be a guide for the subsequent analysis of the spatial structures of climate variables.

2.1 The null hypothesis in time series analysis

It is common in time series to evaluate the spectra of time series against an first order auto-regressive process (AR(1)-process), which goes back to the stochastic climate model of Hasselmann (1976). In its simplest form, Hasselmann's model is an AR(1)-process, which is defined by the following differential equation for time evolution of any physical variable Φ:

$$\frac{\mathrm{d}}{\mathrm{d}t}\Phi = c_{\mathrm{damp}} \cdot \Phi + f \tag{1}$$

with $c_{\mathrm{damp}} < 0$ being a constant damping and f white noise. The auto-correlation function in time, $c(\tau)$, of Φ is:

$$c(\tau) = e^{-\tau/t_0} \tag{2}$$

with the time lag τ and the e-folding time $t_0 = 1/c_{\mathrm{damp}}$. One can derive the analytical form of the spectral distribution of the null hypothesis of Φ from Eq. 2. In time series analysis, this null hypothesis is often used to evaluate the temporal behavior of Φ, by simply comparing the spectrum of Φ with that of a fitted AR(1)-process. The parameters of the fitted AR(1)-process are derived from the auto covariance function of Φ (e.g. Reynolds 1978; Dommenget and Latif 2002b).

In the case of the El Niño SST time series, for instance, the spectrum shows some characteristic enhanced variance (peak) in the interannual frequency range, which is usually interpreted as an indication for the oscillating nature of El Niño SST. The spectrum of the midlatitudes SST time series shows no peak, but a different overall slope of the spectrum, which indicates deviations from the AR(1)-process null hypothesis (Dommenget and Latif 2002b).

2.2 Definitions of teleconnection/climate modes and their limitations

The way EOFs modes are discussed in most statistical analyses (e.g. Dommenget and Latif 2002a and refer-

ences therein) is based on a factor analysis approach, as pointed out by Jolliffe (2003). It is implicitly assumed that the multivariate data $\mathbf{X}$ is a result of the time evolution of a set of K fixed factors, π_i, (often called teleconnections, modes or patterns), and some residual unstructured noise ξ.

$$\mathbf{X}(t) = \Psi(t)\Pi + \xi(t) \tag{3}$$

Π is a matrix of factor loadings π_i, where each π_i is interpreted as a coherent spatial pattern (teleconnection). These patterns are the dominating influence for $\mathbf{X}$ (for details on factor analysis see textbook by Jolliffe 2002). The time evolution of Π is given by a matrix of time series Ψ.

The idea is to assume that the high-dimensional system can be approximated by a low-order state space model, with the number of modes, K, much smaller than the dimension of $\mathbf{X}$ (von Storch and Zwiers 1999, Sect. 15.5). The patterns Π in this approach are a reflection of the underlying low-order physical model. This approach, however, depends strongly on how the patterns Π are estimated. In the recent literature it seems a popular approach to associate the leading EOFs or other statistical modes with the leading teleconnections (e.g. Thompson and Wallace 1998 or Saji et al. 1999). It is, however, important to note that it is in general unclear if any teleconnections exist in the data set and how they can be estimated (e.g. Jolliffe 2002, Sect. 7 and Dommenget and Latif 2002a). Dommenget and Latif (2002a) argue that most likely neither EOF nor VARIMAX will find the leading teleconnection factors in climate data sets. The inherent problem in this approach is that a criteria or algorithm needs to be formulated by which the empirical patterns Π are chosen. Thus the resulting modes may in many cases be a reflection of the statistical method used, but are not a good representation of the underlying physical processes.

An alternative method, which avoids to formulate any criteria for the structure of teleconnection modes, is to formulate a null hypothesis for the structure of spatial variability, which can be regarded as a model for the noise. Any pattern that is very distinct from the patterns of the null hypothesis is a good starting point for the estimation of teleconnection modes. This concept is similar to the time series analysis, in which the time scale behavior of El Niño, for instance, is simplified into a distinct oscillation mode on interannual time scales and a background red noise. In analogy the teleconnection modes are defined as the modes that stick out of the background noise, as define by the null hypothesis.

3 A stochastic null hypothesis for the spatial structure of climate variability

The stochastic model of Calahan et al. (1996) is essentially given by the correlation between two spatial locations of the data field, Φ:

$$c(r) = e^{-r/d_0} \tag{4}$$

Here r is the distance between the two locations and d_0 is the decorrelation length. Note that Eq. 4 is the equivalent to Eq. 2. Thus the stochastic model of Calahan et al. (1996) is an AR(1)-process in the spatial domain dimension.

The simple physical model in Eq. 1 can be extended to include diffusion for the relation between two locations:

$$\frac{\mathrm{d}}{\mathrm{d}t}\Phi = c_{\mathrm{damp}} \cdot \Phi + c_{\mathrm{diffuse}}\nabla^2\Phi + f \tag{5}$$

c_{diffuse} is a diffusion coefficient and f now represents spatial and temporal white noise. In this equation the diffusion is just introduced in a statistical sense. This diffusion model is often refered to as a simple energy balance models of the climate system (see e.g. North et al. 1981, 1983 and references there in). Leung and North (1991) discussed some statistics of this model for the atmospheric variability of a zonally symmetric planet. North (1984) finds that the EOFs of this model driven by homogenous forcing f (spatially white noise with the standard deviation of f constant over the domain) coincide with the eigen modes of the dynamic operator of the system.

Note that for an isotropic diffusive process (neither c_{damp} nor c_{diffuse} are a function of the location) driven by a homogenous forcing f, the model in Eq. 5 is an AR(1)-process in the spatial domain. We can derive the covariance matrix of Φ:

$$\Sigma_{ij} = \sigma_i\sigma_j e^{-d_{ij}/d_0} \tag{6}$$

where σ_i is the standard deviation of Φ at point i and d_{ij} the spatial distance between the two points i and j. If the standard deviation field σ or d_0 exhibit spatial variations (e.g. $\sigma_i \neq \sigma_j$ *for* $i \neq j$), than the model in Eq. 5 is not a spatial AR(1)-process any more and Eq. 6 does not exactly represent the covariance matrix of Φ. However, Eq. 6 should be a good approximation if the spatial variations of σ_i and d_0 are small. The effect of spatial variations of σ will be discussed in Sect. 5 by means of a realistic example.

An isotropic diffusive process in Eqs. 5 and 6 is the null hypothesis for the spatial characteristics of a

climate variable Φ. In this formulation, Φ has no teleconnections other than the exponential decay of its auto-correlation function. In analogy, the spectrum of a time series of an AR(1)-process, is not considered to have a significant time scale (peak in the spectrum) other than a damping time scale.

We can find the EOF modes and eigenvalues of the null hypothesis numerically. In Fig. 1 the leading EOF modes of a domain defined by 17 $\times$ 11 points with constant $\sigma = 1$ and $d_0 = 4.6$ points is shown. The eigenvalues of the leading EOF modes are also shown in Fig. 1.

Based on this example and a few other examples with variations in the domain dimensions and d_0 (not shown), a few important characteristics of the EOF modes and eigenvalues of the diffusion null hypothesis can be formulated as follows:

- The EOF modes are a hierarchy of multi poles, starting with a monopole as EOF-1, followed by a dipole, and then by higher order multi poles. The order and structure of the multi poles is a result of the domain dimensions and the decorrelation length d_0. Note that this kind of structure of the observed leading EOF modes of most climate data sets is also discussed in Richman (1986), but not in the context of the simple stochastic model in (5).
- The EOF-1 peaks in the center of the domain, because the center point is the point which is in average closest to all other points and has therefore a larger covariance with all other points. Note that σ and d_0 are identical for all points, so that the statistics of all points of the domain are identical. The EOF-1 mode is therefore only a reflection of the domain geometry. It simply reflects that there is no structure in the variability other than exponential decay of covariance with distance.
- None of the EOF modes represent teleconnections (factors), since no teleconnections exist in this simple model. In the simple model of an spatial AR(1)-process the spatial variability is a continuous spectrum of spatial patterns, where no spatial pattern is dominating over the other patterns. The EOF modes should be interpreted as a reflection of different spatial scales. In analogy, the spectral coefficients of a continuous spectrum of an AR(1)-process are a reflection of the different time scales, but not a representation of an oscillating behavior. The domain wide monopole of the leading EOF-1 represents the largest spatial scale of variability in the domain, which in an AR(1)-process has the largest variance. EOF-2 and EOF-4, for instance, should be interpreted as spatial variability along the x-axis with a spatial length scale of about 1/2 of the domain size along the x-axis. They do not represent an anti correlation between the centers. The same holds for all other EOF modes.

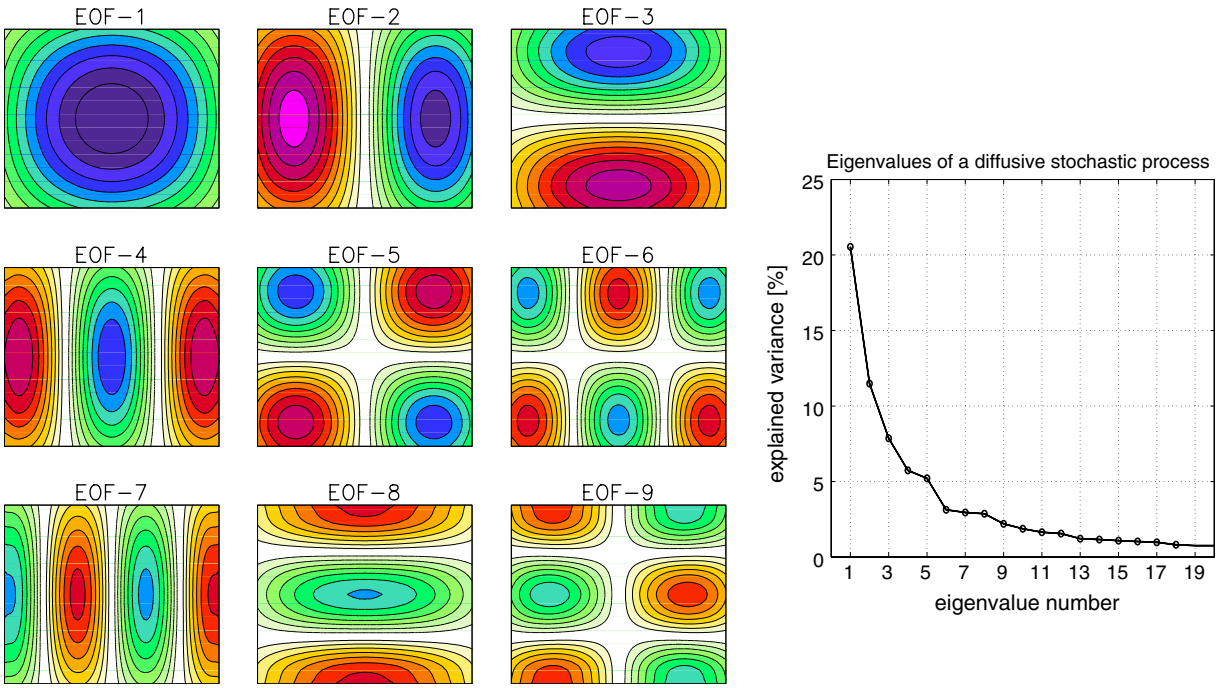

Fig. 1 The leading EOF modes (*left panels*) and eigenvalues (*right panel*) of a spatial AR(1)-process in a 17 $\times$ 11 points domain

- The decrease of the eigenvalues to higher order EOFs is only a function of the domain size and the decorrelation length d_0. None of the 20 leading eigenvalues is degenerated (equal to another eigenvalue), reflecting the different length of the domain along the x- and y-axis. Note that in this example the number of points in each direction was chosen as a prime number to avoid degenerated eigenvalues, which in real domains, such as ocean basins, would not occur. Note also that the numerical precision of the EOF analysis in this example is much better than the line (dot) thickness in Fig. 1.

An important quantity that quantifies the degree of complexity in the domains spatial variability is the effective spatial number of degrees of freedom N_{eff} (Bretherton et al. 1999). It essentially estimates the effective dimension of the multivariate variability:

$$N_{\text{eff}} = \frac{1}{\sum e_i^2}, \quad \text{with} \quad \sum e_i = 1 \tag{7}$$

with e_i the eigenvalues as derived from the EOF analysis. The number N_{eff} corresponds to the number of independent spatial modes. It also quantifies the decrease of the eigenvalues and is a monotonic function of the decorrelation length d_0. It can therefore also be used as an estimate for the decorrelation length.

4 Evaluating EOF-vectors and eigenvalues against a stochastic null hypothesis

The stochastic model allows an evaluation of EOF modes. In many studies only the leading EOF modes of an observed data set are discussed. Here the focus is often on the spatial structure of the observed EOF patterns, which are interpreted as teleconnection patterns. It is therefore important to discuss to which degree the leading EOF modes are consistent with the simple null hypothesis or, in a more objective approach, to find those patterns, that are most distinguished from those of the null hypothesis.

4.1 Fitting an isotropic diffusion process to data

The null hypothesis as formulated in the previous section can be fitted to any data set by estimating the standard deviation field σ and the average decorrelation length d_0. Given σ and d_0 the covariance matrix of the null hypothesis in Eq. 6 is defined and the EOF modes of the null hypothesis can be calculated.

Note that the estimation of d_0 can have large uncertainties in a limited gridded domain (see e.g. von Storch and Zwiers 1999). However, d_0 is a monotonic function of the spatial number of degrees of freedom, N_{eff}, which is estimated by the sum of eigenvalues. The estimation of d_0 will usually depend on the correlation of neighboring points, which is a function of the variability on all spatial scales. The estimation of N_{eff} is essentially a function of the leading EOF-modes only, while the small scale variability has little effect on this quantity. Hence, the agreement between the leading eigenvalues of the observations and the fitted null hypothesis appears to be better if the observed N_{eff} is used to estimate the fitted d_0 in Eq. 6. An analytical relation between N_{eff} and d_0 may exist for some simple domain geometries, such as a sphere for instance. However, it will be difficult to write down an analytical relation for complicated geometry and boundary conditions and it may therefore be most practical to estimate these quantities numerically. Thus, d_0 is varied until N_{eff} of the fitted null hypothesis agrees with the N_{eff} of the observational data set within the uncertainty range of N_{eff}, which should be given by the statistical uncertainties of the eigenvalues due to sampling errors (North et al. 1982).

4.2 Comparing the observed EOF modes with a null hypothesis

An EOF eigenvector (mode) of an observed data set, $\vec{E}_i^{\text{obs}}$, and the corresponding eigenvalue e_i^{obs} can be compared to the eigenvectors $\vec{E}_j^{\text{null}}$ and eigenvalues e_j^{null} of a null hypothesis by projecting the eigenvectors $\vec{E}_j^{\text{null}}$ onto the eigenvector $\vec{E}_i^{\text{obs}}$.

$$c_{ij} = \frac{\vec{E}_i^{\text{obs}} \vec{E}_j^{\text{null}}}{|\vec{E}_i^{\text{obs}}||\vec{E}_j^{\text{null}}|} \tag{8}$$

c_{ij} is the uncentered pattern correlation coefficient between the two EOF-patterns. The variance that the mode $\vec{E}_i^{\text{obs}}$ would have under the null hypothesis can be estimated by the linear combination of all eigenvalues e_j^{null} of the null hypothesis using c_{ij}:

$$e_i^{\text{obsnull}} = \sum_{j=1}^{N} c_{ij}^2 e_j^{\text{null}}. \tag{9}$$

The variance e_i^{obsnull} is the expected variance of $\vec{E}_i^{\text{obs}}$ if the data follows the diffusive process of the null hypothesis. Note that while the eigenvalues e_i^{obs} decrease monotonically with higher order numbers, the e_i^{obsnull} values does not need to decrease with higher order number. A pattern that explains a lot of variance

in the observations (large e_i^{obs}) may explain little variance under the null hypothesis (small e_i^{obsnull} values).

4.3 Statistical inferences about the nature of EOF modes

The uncertainties of the eigenvalues e_i^{obs} of the observed data due to sampling errors are given by North et al. (1982). When the observed data follows the null hypothesis we expected the e_i^{obsnull} value to be within the uncertainties of the eigenvalues e_i^{obs}. A comparison of the eigenvalue spectrum e_i^{obs} with the spectrum of e_i^{obsnull} allows to quantify the deviations of the observed data from the null hypothesis, which can be the basis for statistical inferences about the nature of EOF modes. The concept is in analogous to the comparison of the spectrum of an observed time series with the spectrum of the fitted AR(1)-process.

e_i^{obs} and e_i^{obsnull} are variances, which tend to be χ^2-distributed. Statistical inferences about χ^2-distributed random variables are usually obtained on the basis of the ratio, $e_i^{\text{obs}}/e_i^{\text{obsnull}}$, as in time series analysis (e.g. Reynolds 1978; Dommenget and Latif 2002b). However, as mentioned in Calahan et al. (1996), the strongest deviations of the ratio, $e_i^{\text{obs}}/e_i^{\text{obsnull}}$, are found in the low (higher order) eigenvalues, which are in most studies of little interest. It therefore may be more instructive for large-scale teleconnections to base the statistical inferences on the difference between e_i^{obs} and e_i^{obsnull}. However, the choice of the right test variable depends on the focus of the analysis.

The method of projecting the null hypothesis onto observed patterns can be used for all kind of patterns, like box-averages or more sophisticated indices. The explained variance of the index compared to the explained variance e_{obsnull} could reveal whether the index indeed presents an unexpected structure and thus can be used to justify a specific choice of indices.

5 DEOFs: An estimate of teleconnection modes

If the $\vec{E}_{\text{obs}}$ appear to be different from the null hypothesis one may be interested in the spatial pattern that maximizes the difference in explained variance between the data and the null hypothesis. These are named distinct EOFs (DEOFs or $\vec{D}^{\text{obs}}$) and distinct PCs for the time series (DPCs), respectively. The leading $\vec{D}^{\text{obs}}$ is defined as the pattern that maximizes the differences in explained variance Δ_{var}:

$$\Delta_{\text{var}} = \text{Var}_{\text{obs}}(\vec{D}^{\text{obs}}) - \text{Var}_{\text{null}}(\vec{D}^{\text{obs}}) \tag{10}$$

where Var_{obs} denotes the variance that the pattern $\vec{D}^{\text{obs}}$ explains in the observed data and Var_{null} denotes the variance that the pattern $\vec{D}^{\text{obs}}$ explains under the null hypothesis following (9) The leading $\vec{D}^{\text{obs}}$ can be found by pairwise rotation of the leading EOFs, as it is done for determining the VARIMAX modes (Kaiser 1958), until the maximum of Δ_{var} is found. By iterating this procedure we can define a complete set of orthogonal DEOFs, building a complete representation of the data.

The patterns that are most distinguished from the null hypothesis, the leading DEOFs, are, from a statistical point of view, a good first guess for the teleconnections. They should in general be a good starting point for the understanding of the underlying physical processes.

The DEOF have, however, some limitation in the interpretation, that are similar to those pointed out for EOFs in Sect. 3. Identifying the DEOFs with coherent teleconnections depends on the formulation of the null hypothesis. Furthermore, the concept of teleconnection patterns may not always be helpful in the understanding of the multivariate data. In some systems, for instance, the DEOFs are a reflection anisotropy in the diffusion or advection, which are better described by physical process parameter. Coherent teleconnection patterns may not exist in such systems. The DEOFs focus on the deviations in the leading (large) eigenvalues, while differences in the higher order (small) eigenvalues are neglected, which in some systems may be important for the understanding of the underlying physical processes (Crommelin and Majda 2004).

The DEOF are defined in an orthogonal system, which, similar to EOFs, maximize some variance criteria. Therefore it can be difficult to interpret the DEOFs in systems where many DEOFs explain more variance than expected under the null hypothesis (see also the discussion of the observed Northern Hemisphere and tropical SLP variability in Sects. 5.5, 5.6 and 6).

Note that due to the limited length of the time series the expected value of Δ_{var} is larger then zero, when the data follows the null hypothesis. For statistical inference about the significance of Δ_{var} of the leading DEOF we have to estimate the probability distribution function (PDF) of Δ_{var}. The simplest way to estimate the PDF of Δ_{var} of the leading DEOF is by means of a bootstrapping approach (see von Storch and Zwiers 1999).

6 Examples

We start with some artificial examples, in which the true nature of the problem is well defined. The two artificial examples illustrate two different ways in which a multivariate data set can differ from a pure isotropic diffusion process. We shall then discuss several examples of observed climate variability, some of which have led to some controversy in the recent literature. In the discussion of all examples, the null hypothesis of the climate variability is an isotropic diffusion process as formulated in Sect. 3 and the parameters are fitted to the data as described in Sect. 4.1. The discussion of the observed climate variability modes will be brief and focuses on the new technique. A more detailed physical analysis of the observed climate variability modes may be desirable, but would be beyond the scope of this paper.

6.1 An isotropic diffusive field with inhomogeneous standard deviation

The following example is a numerical stochastic realization of Eq. 5, which should be similar in its statistics to typical monthly mean time series of ocean basin SSTs. The model in Eq. 5 was integrated on a grid with 18×18 points with a daily time step. The diffusion coefficient was chosen to produce a decorrelation length of about 3 points. For the statistical analysis, 30 time steps were averaged to build a monthly mean and the damping c_{damp} in Eq. 5 was chosen to create a one month lag correlation of about 0.6. The resulting time series has a length of 1,000 months with about 500 degrees of freedom. The standard deviation of the spatially uncorrelated forcing f was increased in two regions, with one peak in the northeast and one in the southwest. The resulting standard deviation of Φ varies between 1.0 and 4.0 (at the peaks) in arbitrary units. The EOF analysis was performed on only the central 10×10 domain to avoid boundary effects.

In Fig. 2a–c, the leading EOFs of the stochastic simulation are shown. In addition, the leading EOFs of the covariance matrix Σ based on Eq. 6 with parameters σ_i and d_0 fitted to the statistics of the simulation are shown for comparison (Fig. 2d–f). The explained variance of the EOF modes of the simulation, e_i^{obs}, are compared with the fitted isotropic diffusion process by projecting the EOF modes of the null hypothesis onto the EOF modes of the stochastic simulation as outlined in Sect. 4 using Eqs. (8) and (9) (see Fig. 2g). Note that while the eigenvalues e_i^{obs} decrease monotonically with higher order numbers, the variance under the null hypothesis, e_i^{obsnull}, does not need to decrease with higher order number, because these are not eigenvalues (see section 4.2).

In a first comparison we find that the EOF modes and eigenvalues of the stochastic simulation are in good agreement with the fitted null hypothesis. If we rotate towards the leading vectors $\vec{D}^{\text{obs}}$, which point towards the largest differences, the two leading modes (see Fig. 2h, i) reveal some significant structures (no other higher order mode shows any significant differences). These two structures represent some differences in the spatial scale of variability near the two centers of the leading EOF mode. They reflect that Eq. 6 is only an approximation if structures in σ or d_0 exist. In this example the structure introduced in the standard deviation of the white noise forcing f leads to some structure in the standard deviation of Φ and it also creates some variations in d_0. However, the difference between the stochastic simulation and the null hypothesis amounts to only 4% for the leading mode.

If we repeat the experiment with a homogenous standard deviation of the forcing f, the significant structure in the leading vectors $\vec{D}^{\text{obs}}$ is gone (the difference in explained variance is $< 2\%$, decreasing with the length of the time series).

In summary, the EOF modes and eigenvalues are close to those of the null hypothesis.

6.2 A diffusive field with a weak teleconnection pattern

Here the standard deviation of the forcing f is homogeneous through out the domain. In addition to the spatially and temporally white noise forcing f, a teleconnection forcing pattern π was introduced in Eq. 5 leading to the following equation:

$$\frac{\mathrm{d}}{\mathrm{d}t}\Phi = c_{\text{damp}} \cdot \Phi + c_{\text{diffuse}} \nabla^2 \Phi + \pi \cdot F + f \tag{11}$$

The spatial pattern of π is shown in Fig. 3a, where F is a white noise time series with a variance of about 12% of the variance of f. The teleconnection forcing pattern π is therefore relatively weak. Figure 3b, c highlights the correlation between the two centers of the teleconnection forcing pattern by means of box correlations, showing only a weak correlation in Φ between the two centers. For the EOF analysis, the data were normalized so that each point has unity standard deviation. As a result the stochastic simulation reflects a domain which has no structure in the standard deviation of Φ, but it has a structure in the covariance matrix forced by a teleconnection pattern.

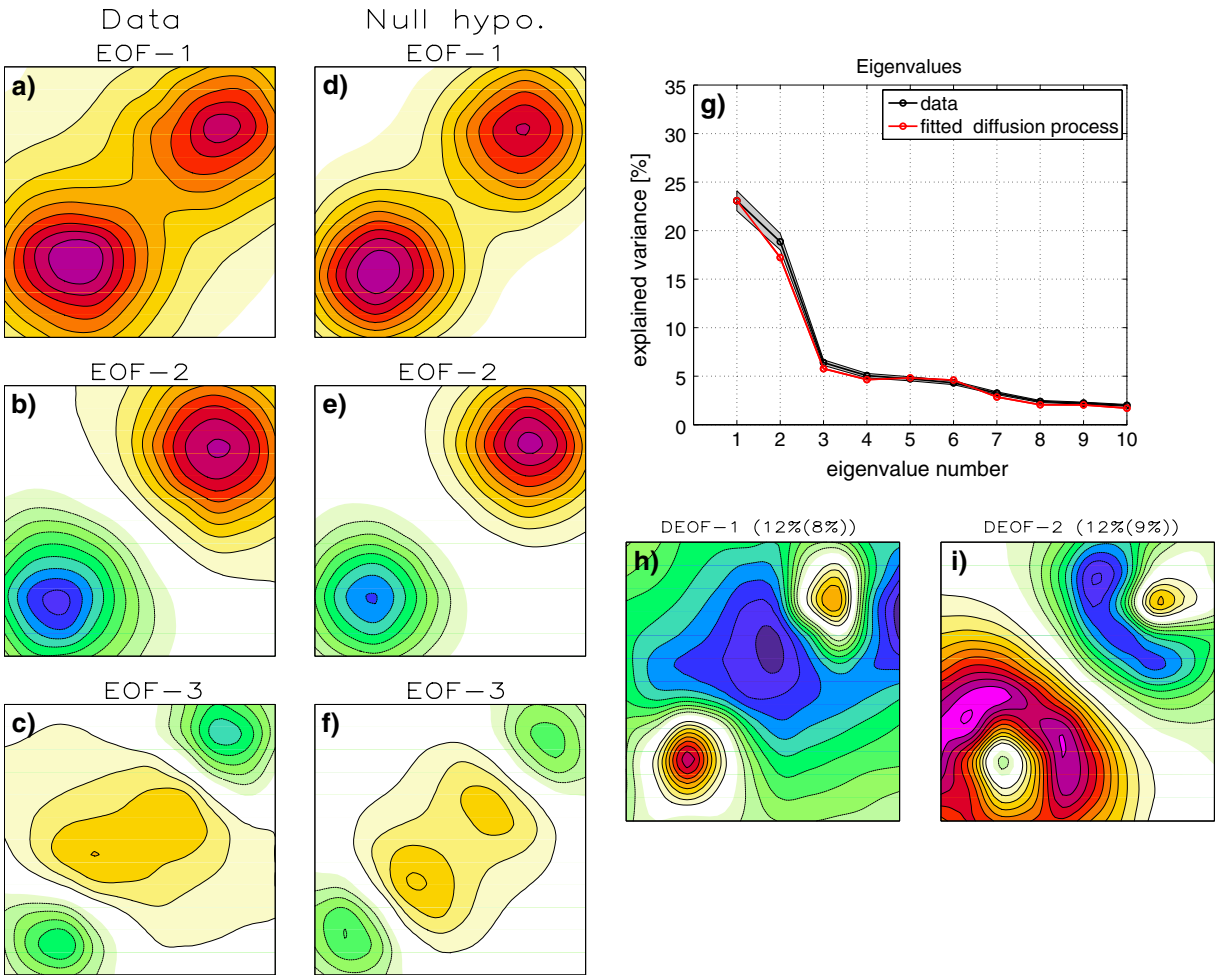

Fig. 2 The leading EOFs of the stochastic simulation (**a**–**c**) and the EOFs of the fitted isotropic diffusion process (**d**–**f**) of the example in Sect. 5.1 are shown. The eigenvalues e_i^{obs} (*black line*) are compared with the projection of the fitted diffusion process e_i^{obsnull} (*red line*) in **g**. The shaded envelope around the black line is the statistical uncertainty of the eigenvalues e_i^{obs} due to sampling errors after North et al.(1982). **h** and **i** show the leading DEOF-1 and DEOF-2. The first percentage value in the heading of the **h** and **i** give the explained variance of the DEOF in the stochastic simulation and the second value the explained variance of the DEOF under the null hypothesis. All spatial modes are in arbitrary units. *Dashed contours* indicate negative values

The EOF modes and eigenvalues are shown in Fig. 3d–k. The EOF modes are very similar to those of a purely diffusive process as discussed in Sect. 3, but the eigenvalue of EOF-2 is larger than expected by a diffusive process. The leading mode of the rotation towards the largest difference relative to the fitted isotropic diffusion process, DEOF-1, is very similar to the teleconnection forcing pattern. DEOF-1 explains 18% of the total variance, where this pattern would only explain 10% in the fitted AR(1)-process (see Fig. 3l). Thus the residual of about 8% of the total explained variance may be associated with a teleconnection following the spatial structure of DEOF-1. Note that none of the leading VARIMAX modes (not shown) have any similarity to the teleconnection π, because the structure of the teleconnection forcing pattern (a dipole) does not maximize the VARIMAX criteria 'simplicity'.

6.3 Tropical Pacific SST

The first example of observed data is the tropical Pacific (from 30°–30°N to 100°E–70°W) monthly mean SST as presented by the HADISST data set from 1870 to 2003 (Folland et al. 1999). The ENSO mode in the tropical Pacific is probably the best understood teleconnection mode of natural global climate variability and is therefore a good example on which to apply the analysis introduced in this paper. Whether or not the ENSO mode is stochastically forced, as assumed by

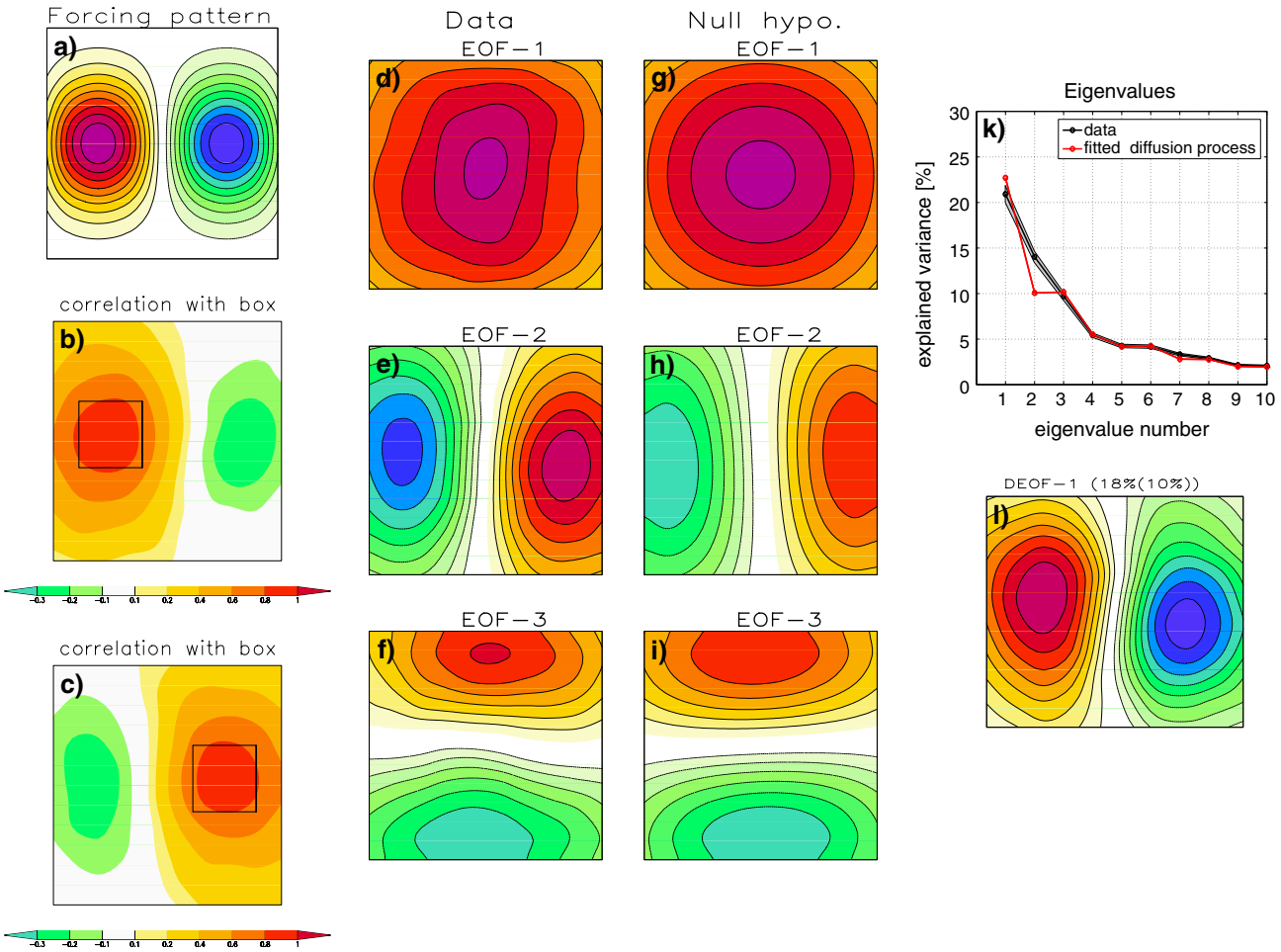

Fig. 3 As in Fig. 2 but for the example in Sect. 5.2. In addition the forcing pattern π is shown in **a**, and the box-average correlations of two regions with the rest of the domain are shown (**b** and **c**)

the null hypothesis, or is due to intrinsic chaotic behavior, will not be addressed in this work (Kirtman et al. 2005 and references therein).

The three leading EOFs are compared with the EOFs of the fitted null hpyothesis in Fig. 4a–f. The structures of the leading EOFs of the observed SST are quite different to those of an isotropic diffusion process. The comparison of the variance of the eigenvalues shown in Fig. 4g clearly shows that nearly all leading EOFs are different from the null hypothesis.

If we maximize the difference between the observed EOF modes and the null hypothesis by rotation we find a pattern similar to EOF-1 (see Fig. 4h), with less explained variance (32%) but with a much larger difference relative to the null hypothesis of about 22%, which makes this mode more distinct to a diffusive process than EOF-1. It is also interesting to note that the leading teleconnection DEOF-1 is more focused on the central equatorial region than the EOF-1, a region often discussed in ENSO forecasting studies to be the most predictable region on seasonal to interannual time scales (e.g. Barnett et al. 1993; Dommenget and Stammer 2004).

6.4 Tropical Indian Ocean SST

The EOF-1 of the monthly mean Indian Ocean SST (20°S–30°N to 30°E–120°E) from the HADISST data set over the period from 1870 to 2003 (Folland et al. 1999), as shown in Fig. 5a, has been identified as the response of the Indian Ocean to ENSO by Saji et al.(1999). They further identify the EOF-2 as a new mode of ocean–atmosphere interaction in the Indian Ocean. A discussion of whether or not this interpretation is justified can be found in Baquero and Latif (2002), Behera et al. (2003) and in Dommenget and Latif (2003).

The spatial structure of the leading EOFs appear to be very similar to the EOFs of the null hypothesis and the leading eigenvalues are in good agreement with the

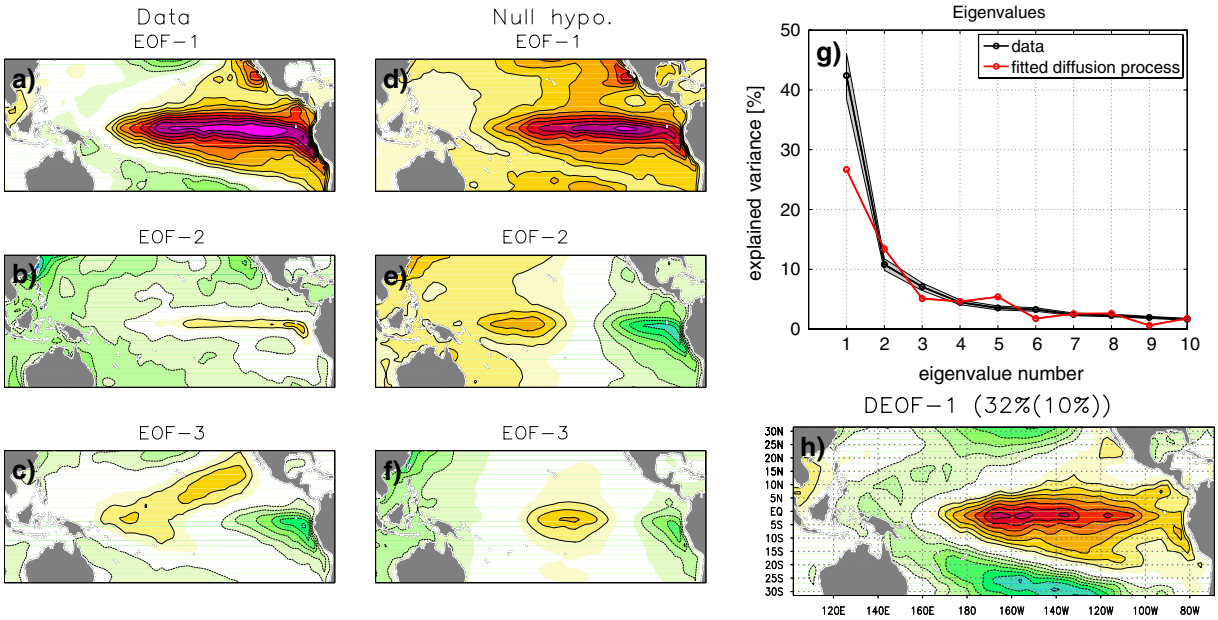

Fig. 4 As in Fig. 2 but for the tropical Pacific SST as discussed in Sect. 5.3

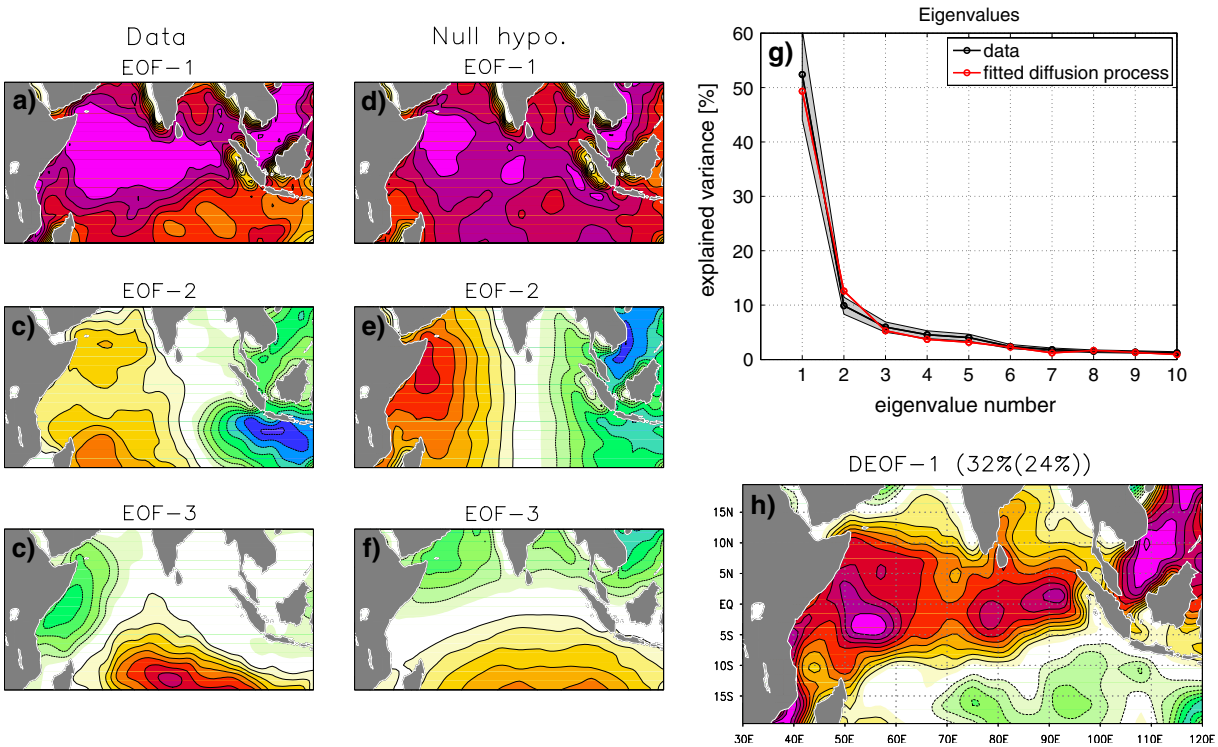

Fig. 5 As in Fig. 2 but for the tropical Indian Ocean SST as discussed in Sect. 5.4

variance of the null hypothesis (see Fig. 5a–g). It therefore seems that the SST variability of the Indian Ocean is consistent with a purely diffusive process. In particular, EOF-2, the so called Indian ocean dipole mode, explains less variance than expected from the fitted AR(1)-process.

Although there is no indication for strong deviations from an isotropic diffusion process, a rotation towards the leading differences from the null hypothesis was performed (see Fig. 5h). However, DEOF-1 explaining 32% of the total variance (24% in the null hypothesis) is only slightly different from the null hypothesis.

6.5 Northern hemisphere winter time SLP

Thompson and Wallace (1998) proposed the Arctic Oscillation (AO) or the annular mode as one of the leading modes of climate variability, which is defined by EOF-1 of Northern Hemisphere (from 10°N) wintertime SLP. The leading EOFs are shown in Fig. 6a–c based on the NCEP SLP from 1948 to 1999 (Kalney et al. 1996). A teleconnection between the Pacific and Atlantic region is seen in EOF-1.

However, Deser (2000) and Ambaum et al. (2001) pointed out that the AO does not project onto local correlation patterns as well as the two more localized patterns of the North Atlantic Oscillation (NAO) and the Pacific North America pattern (PNA), which are the leading EOFs of the Atlantic and Pacific sub domains. The NAO and the PNA both project well onto the AO pattern. Further, they argue that the data does not give much support for strong interactions between the Atlantic and Pacific region as the AO pattern suggests.

In response to the lack of correlation between the two oceans, Wallace and Thompson (2002) argue that the EOF-2 may represent another inter-oceanic mode of variability, which leads to the apparent weak correlation between the SLP over the two oceans. In summary, Thompson and Wallace indicate that there is a relatively strong connection between the Atlantic and Pacific regions, whereas Deser (2000) and Ambaum et al. (2001) do not see evidence for this connection.

Furthermore, the arguments of Deser (2000) and Ambaum et al. (2001) are similar to the arguments which lead to the null hypothesis. Assuming the leading modes of variability should be reflected in the local correlation patterns, as the two more localized patterns NAO and PNA, is in principle the same as assuming that the data are dominated by diffusive processes and a few (one or two) teleconnections.

The leading EOFs of observed wintertime SLP are quite different from those of the null hypothesis in that each of the leading EOFs explains considerably more variance than it would under the null hypothesis (see

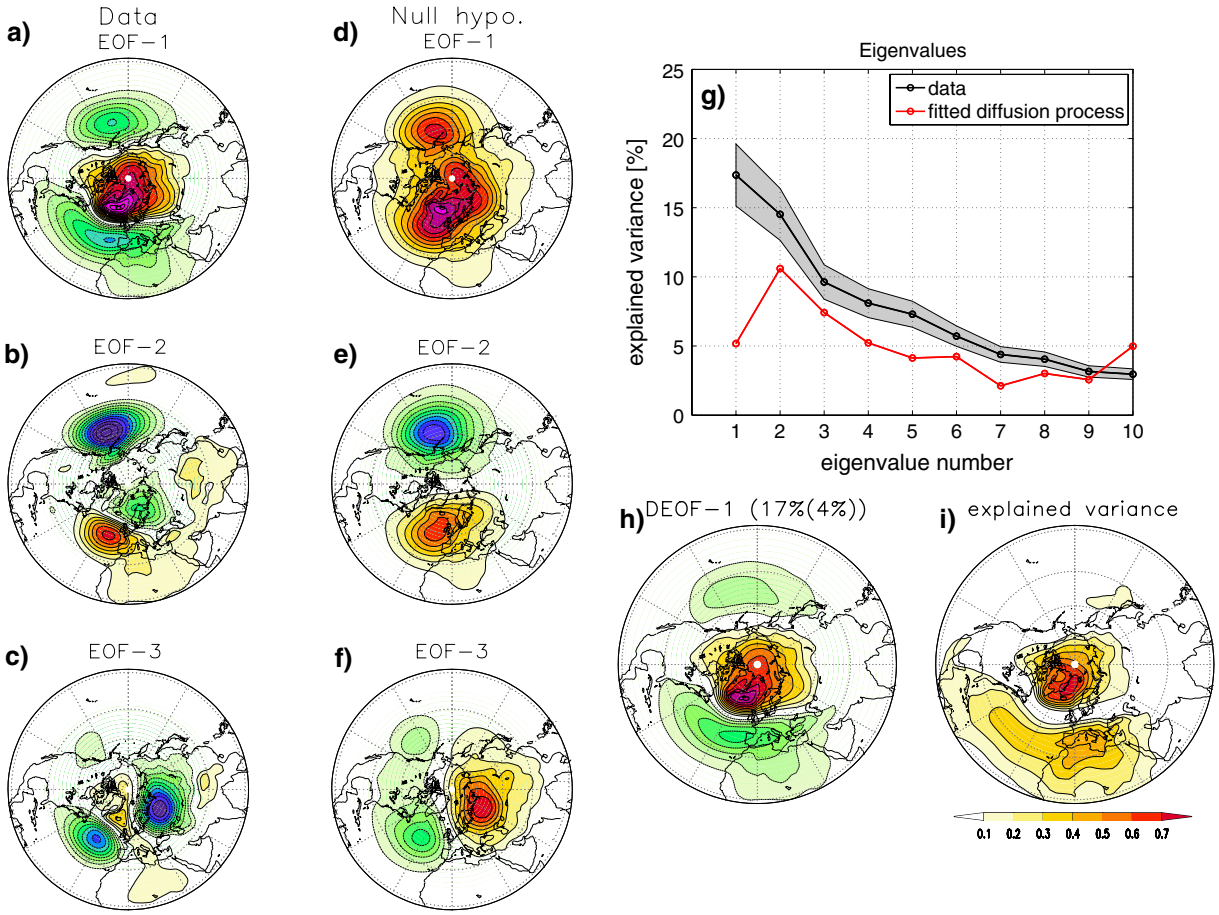

Fig. 6 As in Fig. 2 but for the Northern Hemisphere wintertime SLP as discussed in Sect. 5.5. In addition the explained variance field of DEOF-1 is shown (**i**)

Fig. 6a–g). The comparison therefore indicates that the wintertime SLP is inconsistent with diffusive processes. However, the leading teleconnection DEOF-1 is quite clearly represented by a NAO like structure explaining about 17% (4% in the null hypothesis) of the total variance (see Fig. 6h, i). Note that this pattern has a high correlation with the EOF-1 or AO mode, but it explains very little variance in the Pacific region (see Fig. 6i).

Note that one should resist in interpreting all the DEOFs, that explain more variance, than expected under the null hypothesis, as teleconnection patterns. In multivariate systems with many DEOFs explaining more variance than expected under the null hypothesis, the interpretation of the DEOFs can be very difficult and the concept of teleconnection modes may not be very helpful. It may in some cases be possible to identify some of the DEOFs with teleconnections, but one have to keep in mind that in a multivariate orthogonal system, rotation of the dominant DEOFs patterns may lead to a different presentation of the leading teleconnections. Moreover, the DEOF will in most cases not represent any coherent teleconnections, but be a reflection of dominant physical process that drive SLP in the extra tropics, such as mass and vorticity conservation.

6.6 Tropical SLP

Tropical monthly mean SLP variability is strongly related to SST variability, which is dominated by the ENSO-mode. While the El Niño SST pattern is well represented by the leading EOF of the tropical Pacific SST, the Southern Oscillation mode is not well represented by the leading EOF of the tropical SLP, see Fig. 7a. The Southern Oscillation has some similarity with EOF-2, but is usually defined by the correlation with the NINO3 region (5°S–5°N/150°W–90°W) or as the pressure difference between the stations at Darvin and Tahiti.

The structure of the EOF-patterns is similar to what is assumed for a pure isotropic diffusion process (as discussed in Sect. 3), with a monopole as EOF-1 followed by dipole patterns in EOF-2 and EOF-3. Thus the structure or the EOF-patterns does not suggest any characteristic teleconnection pattern. The important role of the EOF-2 (Southern Oscillation) becomes clear, when the eigenvalues of the EOFs are compared with the fitted null hypothesis (Fig. 7g). Overall the eigenvalues of the EOFs are relatively close to those of the fitted null hypothesis, but the EOF-2 explains considerably more variance than expected, while EOF-3 explains much less variance than expected. The situation is similar to the artificial example with a zonal dipole teleconnection, as discussed in Sect. 5.2.

The leading DEOF is similar to the EOF-2 (Southern Oscillation), but is more global, with larger amplitudes in the tropical Atlantic region. In the context of the ENSO mode we would expect the leading SLP in the tropical atmosphere to be correlated to the SST. The DPC-1 of the tropical SLP shows higher correlations with the PC-1 and DPC-1 of the SST in the tropical Pacific (as discussed in Sect. 5.3) than the PC-2 of the tropical SLP. It also shows larger correlations with global SST than the PC-2 of the tropical SLP, including the North Pacific, tropical Indian Ocean and Atlantic, which are region known to be influenced by the ENSO mode.

The tropical SLP also shows some clear anisotropy in the decorrelation length. In the zonal direction the decorrelation length is much larger than in meridional directions. This deviation from the isotropic diffusion process becomes more dominant in the leading DEOFs, if the analysis is repeated on a wider latitudes range (e.g. 30°S–30°N; not shown). The mismatches between the leading eigenvalues and the fitted null hypothesis become larger, but the EOF-2 (Southern Oscillation) remains to be the largest deviations from the null hpyothesis. The southward shift of the amplitudes in the DEOF-1 (Fig. 7h) is also a reflection of the anisotropy in decorrelation length.

7 Discussion

In this paper it is suggested that the leading EOF modes of observed data are compared with the EOF modes of a fitted stochastic null hypothesis in order to determine what the nature of the spatial structures of the data are. Calahan et al. (1996) formulated a simple stochastic model for rainfall data, which can be used as a general null hypothesis for the spatial structure of climate fields. The stochastic model of Calahan et al. (1996) is an AR(1)-process in the spatial dimension, which is the same as the null hypothesis for the temporal dimension (time series) as introduced by Hasselmann (1976). The spatial AR(1)-process can be described by a simple physical model, in which the relation between two spatial locations is only due to isotropic diffusion. The EOF modes of a spatial AR(1)-process are characterized by a hierarchy of multi poles with decreasing eigenvalues. In this simple model the spatial variability is a continuous spectrum of spatial patterns, where no spatial pattern is dominating over the other patterns.

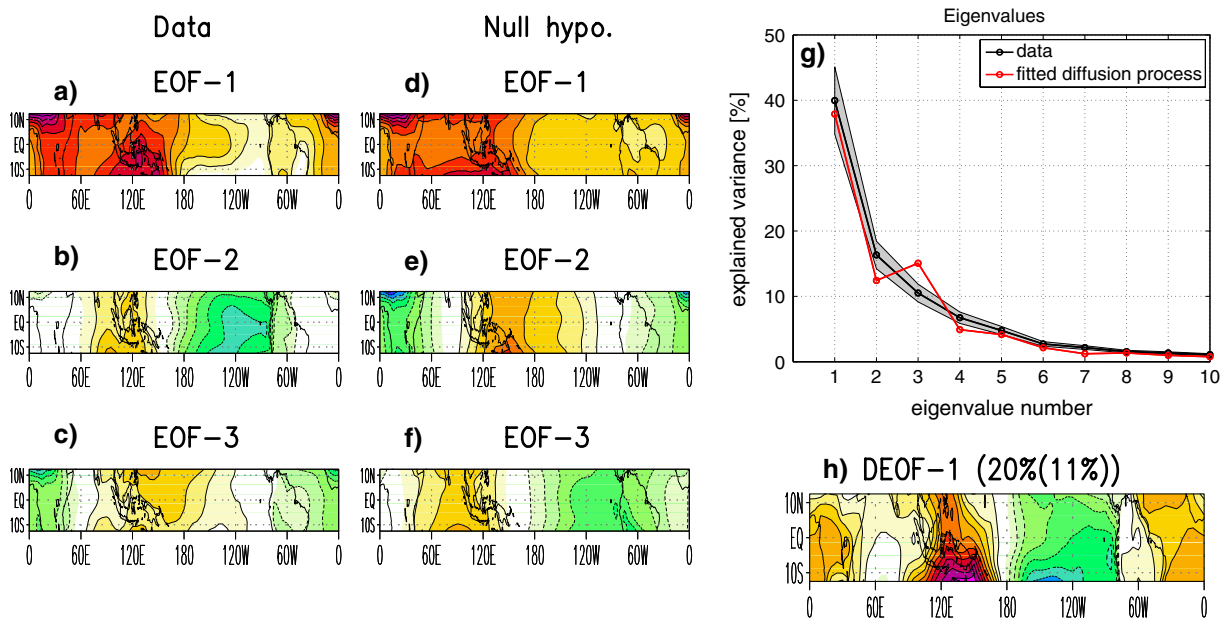

Fig. 7 As in Fig. 2 but for the tropical SLP (from 15°S–15°N to 0°E–360°E)

Similar to time series analysis the formulation of this stochastic null hypothesis for the spatial structure of climate variability allows one to compare the EOF modes and eigenvalues of an observed data set with the EOF modes and eigenvalues of a fitted null hypothesis. It also allows to define a representation alternative to the EOF modes, the so called distinct EOFs (DEOFs or $\vec{D}^{\text{obs}}$). The leading DEOF is defined as the mode that is most distinguished from the modes of the null hypothesis. It represents the direction in the multivariate space, in which the observed data differs most from the null hypothesis, which may be called the ''finger print'' of the observed data. It is a good starting point for the understanding of underlying physical processes. However, one should be careful in interpreting the DEOF as a coherent teleconnection pattern. This will in many cases be a misleading interpretation.

Note that in VARIMAX or other criteria for rotation of the EOFs a simple equation, which reflects a predefined symmetry in the system (e.g. simplicity for VARIMAX), is maximized. The rotation analysis will therefore find patterns that follow the assumed symmetry. The DEOFs introduced in the present study are rotated by comparison with a stochastic null hypothesis, which reflects a physical model. The structure of the resulting DEOF-1 is therefore not predefined by any mathematical symmetry. It is only assumed that it is different from the null hypothesis. It can in some cases point to a coherent teleconnection pattern, but it may also be a reflection of physical processes, different from isotropic diffusion, driving the variability of the domain.

As an example the SST of the tropical Pacific was analyzed, which is known to contain the ENSO teleconnection pattern. The comparison with the fitted isotropic diffusion process clearly supports the idea that the El Niño pattern is the leading teleconnection. The rotation towards the leading differences finds a pattern similar to the EOF-1 but more focused in the central Pacific. It is interesting to note that the EOF-1 mode explains 41% and about 34% in the fitted null hypothesis. Thus about 4/5 of the variance of EOF-1 may be explained by the fitted isotropic diffusion process. The leading rotated mode DEOF-1 explains 32% and about 10% in the fitted null hypothesis. If we consider the diffusive part of the fitted null hypothesis as noise, then the leading DEOF-1 has a much better signal to noise ratio, which amounts to 3:1.

In the other example of the tropical Indian Ocean, the SST seems to be much closer to the fitted isotropic diffusion process.

Northern Hemisphere winter time SLP showed that SLP variability is not well described by a pure isotropic diffusion process. Essentially the entire large-scale structure of Northern Hemisphere SLP deviates from the modes of the fitted null hypothesis. This is somehow not surprising since the large-scale SLP is driven by the quasi-geostrophic equations in which the conservation of absolute vorticity and mass plays an important role, forcing wave like structures (Navarra 1993; Metz 1994; Gerber and Vallis 2005). It is there-

fore inappropriate to assume that local box correlations should reflect the leading teleconnections, because this already assumes that the main characteristics of SLP is that of a diffusive process. A better strategy appears to be a formulation of a stochastic null hypothesis based not on the isotropic diffusion, but on the quasi-geostrophic equations or simple linearized models (Navarra 1993; Metz 1994; Gerber and Vallis 2005). Comparing the observed EOF modes against the EOF modes of a stochastic quasi geostrophic model will help to decide if the SLP variability has teleconnections with strong links between the Pacific and Atlantic region.

The SLP variability of the tropical regions is much closer to the null hypothesis, which may reflect that mass and vorticity conservation are less important in the relatively narrow zonal band of the tropics.

In summary, one should compare the observed spatial patterns to those expected from a simple physical model to evaluate their significance. A good starting point is the isotropic diffusion process, which is the equivalent to the AR(1)-process used in time series analysis.

Acknowledgments This work was motivated by fruitful and inspiring discussions with Alexander Gershunov and Thomas Reichler. Comments from Ian Jolliffe and the anonymous reviewers helped to improve this analysis significantly. Furthermore, I like to thank Noel Keenlyside, Mojib Latif, Katja Lorbacher, Oliver Timm, Jörg Wegener and Jürgen Willebrand for comments and proof reading.

References

Aires F, Rossow WB, Chedin A (2002) Rotation of EOFs by the independent component analysis: toward a solution of the mixing problem in the decomposition of geophysical time series. J Atmos Sci 59:111–123

Ambaum MHP, Hoskins BJ, Stephenson DB (2001) Arctic oscillation or North Atlantic oscillation?. J Clim 14:3495–3507

Baquero A, Latif M (2002) On dipole-like variability in the tropical Indian Ocean. J Clim 15(11):1358–1368

Barnett TP, Graham N, Pazan S, White W, Latif M, Flügel M (1993) ENSO and ENSO-related predictability. Part I: Prediction of equatorial Pacific sea surface temperature with a hybrid coupled ocean–atmosphere model. J Clim 6(8):1545–1566

Behera SK, Rao SA, Saji HN, Yamagata T (2003) Comments on 'A cautionary note on the interpretation of EOFs'. J Clim 16(7):1087–1093

Bretherton CS, Smith C, Wallace JM (1992) An intercomparison of methods for finding coupled patterns in climate data. J Clim 5:541–560

Bretherton CS, Widmann M, Dymnikov VP, Wallace JM, Bladé I (1999) The effective number of spatial degrees of freedom of a time-varying field. J Clim 12:1990–2009

Cahalan RF, Wharton LE, Wu M-L (1996) Empirical orthogonal functions of monthly precipitation and temperature over the United States and homogenous stochastic models. J Geophys Res 101(D21):26309–26318

Crommelin DT, Majda AJ (2004) Strategies for model reduction: comparing different optimal bases. J Atmos Res 61:2206–2217

Deser C (2000) On the teleconnectivity of the ''Arctic Oscillation''. Geophys Res Lett 27(6):779–782

Dommenget D, Latif M (2002a) A cautionary note on the interpretation of EOF. J Clim 15(2):216–225

Dommenget D, Latif M (2002b) Analysis of observed and simulated SST spectra in the midlatitudes. Clim Dyn 19:277–288

Dommenget D, Latif M (2003) Reply to Behera et al. 2003. J Clim 16(7):1094–1097

Dommenget D, Stammer D (2004) Assessing ENSO simulations and predictions using adjoint ocean state north GR, 1984 estimation. J Clim 17(22):4301–4315

van den Dool HM, Saha S, Johansson A (2000) Empirical orthogonal teleconnections. J Clim 13:1421–1435

Folland CK, Parker DE, Colman AW, Washington R (1999) Large scale modes of ocean surface temperature since the late nineteenth century. In: Navarra A (ed) Beyond El Nino. Springer, Berlin Heidelberg New York, pp 73–102

Gerber EP, Vallis GK (2005) A stochastic model for the spatial structure of annular patterns of variability and the North Atlantic Oscillation. J Clim 18(12):2102–2118

Hasselmann K (1976) Stochastic climate models. Part I: Theory, Tellus 28:473–485

Jolliffe IT (2002) Principal component analysis, 2nd edn. Springer, Berlin Heidelberg New York, pp 150–166

Jolliffe IT (2003) A cautionary note on artificial examples of EOFs. J Clim 6(7):1084–1086

Kaiser HF (1958) The varimax criterion for analytic rotations in factor analysis. Psychometrika 23:187

Kalnay E, Kanamitsu M, Kistler M, Collins R, Deaven W, Gandin D, Iredell L, Saha M, White S, Woollen G, Zhu J, Chelliah Y, Ebisuzaki M, Higgins W, Janowiak W, Mo J, Ropelewski KC, Wang C, Leetmaa J, Reynolds A, Jenne R, Joseph R, Dennis R (1996) The NCEP/NCAR 40-year reanalysis project. Bull Am Meteor Soc 77(3):437–471

Kirtman BP, Pegion K, Kinter SM (2005) Internal atmospheric dynamics and tropical Indo-Pacific climate variability. J Atmos Res 62:2220–2233

North L (1991) Atmospheric variability on a zonally symetric land planet. J Clim 4:753–765

Metz W (1994) Singular modes and low-frequency atmospheric variability. J Atmos Sci 51:1740–1753

Navarra A (1993) A new set of orthogonal modes for linearized meteorological problems. J Atmos Sci 50:2569–2583

North GR (1984) Empirical orthogonal functions and normal modes. J Atmos Sci 41:879–887

North GR, Cahalan RF, Coakley JA (1981) Energy-balance climate models. Rev Geophys Sp Phys 19:91–121

North GR, Bell TL, Cahalan RF, Moeng FJ (1982) Sampling errors in the estimation of empirical orthogonal functions. Mon Wea Rev 110:699–706

North GR, Mengel JG, Short DA (1983) A simple energy balance model resolving the seasons and the continents: application to the astronomical theory of the ice ages. J Geophys Res 88:6576–6586

Overland JE, Preisendorfer RW (1982) A significance test for pricipal components applied to a cyclone climatology. Mon Wea Rev 110(1):1–4

Reynolds RW (1978) Sea surface temperature anomalies in the North Pacific ocean. Tellus 30:97–103

Richman MB (1986) Review article: rotation of principal components. J Climatology 6:293–335

Saji NH, Goswami BN, Vinayachandran PN, Yamagata T (1999) A dipole mode in the tropical Indian Ocean. Nature 401:360–363

von Storch H, Zwiers FW (1999) Statistical analysis in climate research. Cambridge University Press, Cambridge. ISBN 0 521 45071 3, 494 pp

Thompson DWJ, Wallace JM (1998) The Artic oscillation signature in wintertime geopotential height field and temperature field. Geophys Res Lett 25:1297–1300

Wallace JM, Thompson DWJ (2002) The Pacific center of action of the northern hemisphere annular mode: real or artifact? J Clim 15(14):1987–1991